Design of photonic crystal add-drop filters based on quasi-ring cavities

HARKIRANJEET KAUR*, RAJINDER SINGH KALER, BALVEER PAINAM
Optical Fiber Communication Research Laboratory (OFCR Lab), ECE Department, Thapar University, Patiala 147004, India

In this work, we presented add drop filters design with two dimensional square photonic crystal lattice. The filters are based upon multiple quasi-ring cavities inside the square cavity. The theoretical power transmittance spectra are analyzed using Finite-Difference Time-Domain (FDTD) approach for two alternative add-drop filter (ADF) layouts. The drop efficiency of 95% is achieved with one of the filters having perfect backward drop at the wavelength of 1.48 μm. The minimum spectral width attained is 68 nm. The size of this device is 12.4 μm × 12.4 μm. The reflecting cavities designed in these structures find their application in ultra-compact photonic circuits and bio-sensing circuits as multiple cavities can easily trap the bio-molecules within them.

(Received July 7, 2015; accepted February 10, 2017)

Keywords: Photonic Crystals (PhC), Finite Difference Time Domain (FDTD), Plane Wave Expansion (PWE), Resonating Cavities, Photonic Band gap, Add-drop Filter (ADF)

1. Introduction

In the recent few years, the photonic crystals [1, 2] have provided a potential platform for a wide range of applications in numerous domains. Many optical communication devices such as multiplexers/demultiplexers [3], interleavers [4], filters [5] etc., designed on the photonic crystals have been reported showing high throughputs. Since the photonic crystal devices have made a significant contribution in the areas of compactness, miniature sizes and fast switching etc., many add drop filters (ADFs) are also designed using photonic crystals.

The ADFs are an essential component of various optical circuits such as multiplexers/de-multiplexers, modulators, switches etc. They consist of two straight waveguides, the bus waveguide and the drop waveguide, having resonating cavities sandwiched between them. The ADFs are coupling devices, in which light launched into bus waveguide tunnels through the resonating cavities to drop waveguide and exits through one of its ports. If the light output exits in the direction parallel to the input light, it is known as forward dropping. Whereas if the light exits anti-parallel to that of input light; it is backward dropping. The filters based on resonating cavities are suitable candidates for wavelength division multiplexing (WDM) communications as they provide better drop efficiency for a given size of a structure [6]. The coupled resonators in cascade help in further improving the individual resonator characteristics [7].

Ahmed Taalbi et al. [8] demonstrated the filter characteristics for single-ring and dual-ring configurations based on 2D triangular lattice photonic crystal (PC) silicon rods. The effect of change of radius of coupling rods and change in dielectric of the structure on the resonant modes is also studied in this work. P. Andalib et al. [9] designed the new ultra-compact ADF based on the 2D triangular lattice. The resonator is formed by two coupled curved Fabry-Perot cavities in the glass background. M. Djavid et al. [10] investigated the multi-channel drop filters based on the square lattice. The input power at resonant wavelength deviates to one of the three waveguide exit ports. The maximum drop efficiency of this three drop ports filter at resonant wavelength is 81%.

In the above literature, various add/drop filters based on both triangular and square lattices are discussed. The ADF having dual curved resonator based on triangular lattice [8] shows a trade-off between drop efficiency and size of the structure. In this dual structure, two ring resonators are cascaded vertically to obtain the complete transfer of light towards the drop waveguide. Although, the cascaded device has higher drop efficiency than a single resonator, it increases the size of structure. The Fabry-Perot cavity resonator discussed [9] has drop efficiency of 68% only. However this hexagonal lattice structure has an advantage of larger overlap between the cavities and the other defects due to curved formation of cavities.

The curved resonator trend of Fabry-Perot cavities [9] can be applied to the square photonic crystal lattice also as more subtle defects can be introduced in the orientation angle between two square lattice vectors as compared to

the hexagonal lattice. The Fabry-Perot cavities act as good reflectors that couple the light waves efficiently along the bends and turns. In this paper, we discuss two new ADF configurations based on square photonic crystal lattice. These structures are formed by curved quasi-ring cavities inside a square cavity between the bus waveguide and drop waveguide which resemble the Fabry-Perot cavities. Various defects are introduced at corners of the cavity to reduce the reflection losses. The transmittance spectrum is analyzed and compared for both the configurations. The curved resonating cavities have an advantage of miniature sizes than the introduction of multi-ring resonating structures as latter require two separate resonators in cascade for better coupling.

Our group is currently working on photonic crystal waveguide sensors [11] as well as working on photonic crystal waveguide add drop filters. In present design structure we achieved more promising results with quasi ring resonators within square cavity of photonic crystal with 95% drop efficiency. Reported results compared with the two circular hole with two waveguides drop efficiency of 92.7% [12] and ultra-compact 32 channel drop filter drop efficiency more than 20% [13] and proved to be more. The achieved results may find applications in wavelength-division multiplexing and related techniques.

This paper is organized as follows. In section 2 the simulation set up of the photonic crystal add-drop filters is described. It discusses all line and point defects introduced in photonic crystal layout to form the filters. In section 3, the results of PWE and FDTD simulations are discussed. Section 4 concludes the paper.

2. Simulation setup

We have designed the add drop filters (ADF) on a 2D square lattice in X-Z plane. The silicon rods of refractive index 3.47 are placed in air wafer. The lattice constant for designed ADF is taken in the range of 5.378 µm to 5.382 µm and radius of rod is 0.172 times the lattice constant which varies from 0.925016 to 0.925704 µm. Hence, approximate radius of the silicon rod is 925 nm which is possible to fabricate according to Olmos et al. [14]. Although fabricating air-hole type PhC-based structures look as if much easier than a pillar-based PhC, but the ease of coupling of the pillar structure cause them to beat the air-holes. Since our device requires a high coupling aptitude, we used a pillar-based PhC structure [15]. Two straight waveguides are formed with the introduction of line defects by removing a series of rods. The input waveguide is the bus waveguide and the coupled waveguide is the drop waveguide which outputs the light of a specific wavelength to one of its ports. We have designed the square resonating cavities consisting of two semi curved reflectors as shown in Fig. 1(a) and Fig. 1(b). The input wave is the Gaussian modulated wave.

All the rods marked red in Fig. 1 are defected rods and are displaced from their original positions to form curved cavities. Scatterer rods are added to the selective corners to reduce the reflection losses. The corners facing open ends of the cavities have no scatterer rods. The input is launched into bus waveguide through vertical arrowed input plane at the left end of layout marked with red color. The ports labeled as B, C and D are output ports.

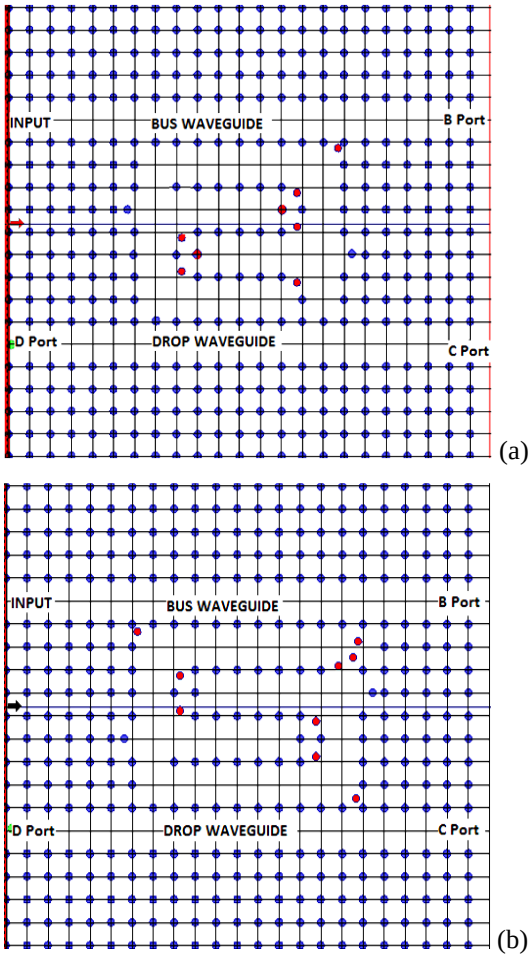

Fig. 1(a). Add drop filter configuration (A). (b) Add drop filter configuration (B)

The square resonating cavity between the waveguides has multiple quasi rings curved inside it as shown in fig. 1(a) and 1(b). The two configurations however differ in the direction of curves formed by the resonating cavities. The cavities in both configurations are facing opposite to each other. These ADFs are designed for backward dropping of the particular wavelength i.e. the light of that wavelength is completely guided towards the D-port of drop waveguide with negligible transmission through B and C port. ADF (A) has lower end terminated to the drop waveguide to enhance backward coupling at the resonant wavelength. Similarly ADF (B) has upper end terminated to the bus waveguide to improve the coupling efficiency. Otherwise the coupled light travelling through this passage suffers high reflection losses at the ends without this termination. The upper end termination thus leads to the smooth transition of light through the bends and turns with minimum losses.

3. Results and discussions

The Photonic Band gap (PBG) for designed ADF devices is calculated using PWE method [16]. The TE modes band gap for the defect-free ADF configurations lies between the range 1/λ (1/μm) equals to 0.5693 - 0.8378, which is the range of wavelengths from 1.193 to 1.756 μm. However, no band gaps are found in TM modes. The k-vector scale is indexed 0-15 in the first Brillouin zone i.e. [0-2π/a] (i.e. any index 'i' corresponds to wave vector (2π/ (15a)* 'i' in reciprocal lattice where 'a' is the lattice constant). This region is a set of non-equivalent wave vectors closest to the k=0. We observe that every dispersion curve in the Fig. 2 has same value of frequencies at the k-vector index equals to 0 and at index equals to 15. This is due to the fact that this region represents non redundant wave vectors following the rotational symmetry. Beyond this region, the same gap structure repeats. Therefore, the ends overlap the dispersion curves at the values the curves started.

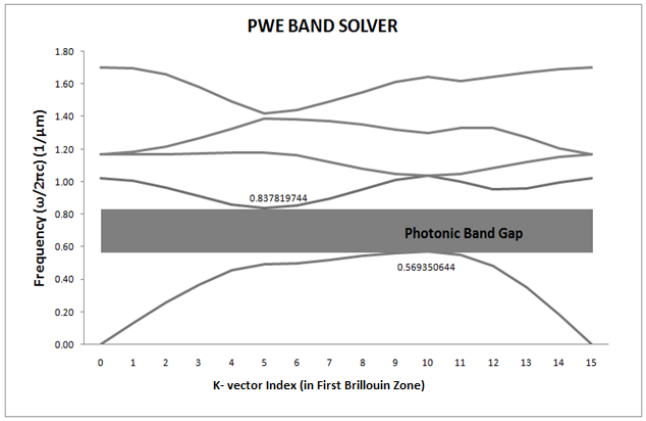

(a)

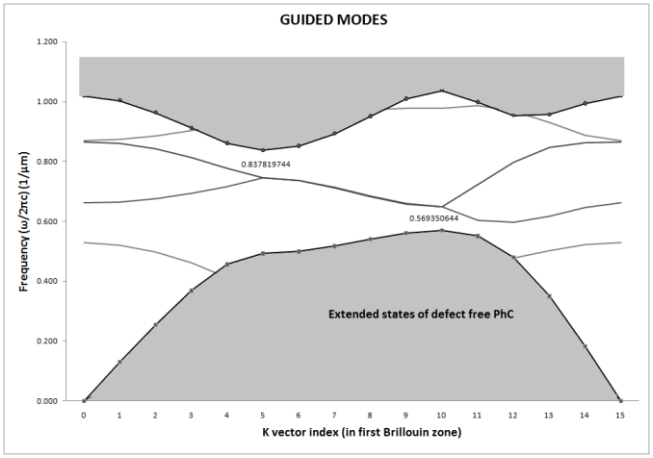

(b)

Fig. 2 (a.) TE modes Photonic Band gap for defect-free photonic crystal. (b.) Guided TE modes of the photonic crystal with line-defects (i.e. the waveguides in the ADF circuits)

The introduction of line defects in the photonic crystal introduces guided modes within the photonic band gap as shown in Fig. 2(b), thus allowing the propagation of light signal along the waveguides in the ADFs given in Fig. 1. Thus, these ADF structures are simulated by launching the input Gaussian wave of 1.5 μm through the vertical input plane as this wavelength of 1.5 μm lies in the band gap and is guided efficiently through the waveguides in ADFs.

The transmission spectrum of the two ADFs are simulated using the FDTD method [17] for the calculation of light transmittance through various output ports at the wavelength of 1.5 μm. Light dropping efficiencies are analyzed by visualizing the transmittance spectra as given below in the Fig. 3 and Fig. 4. In Fig. 3, it shows the electric field distribution (Ey) image maps of the ADF layouts placed in the X-Z plane and Fig. 4 calculates the transmittance spectra curves showing the power distribution for both the layouts.

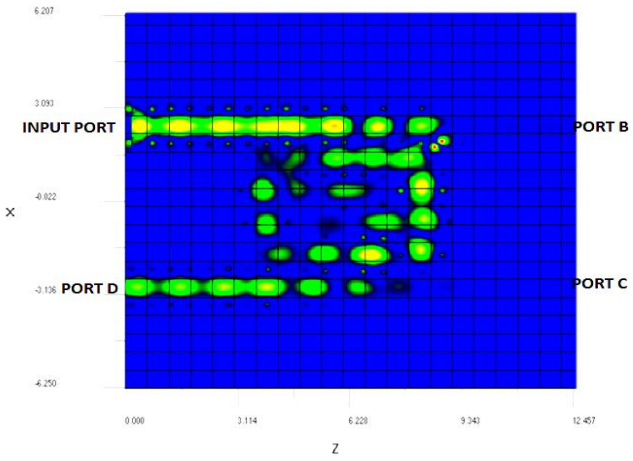

(a)

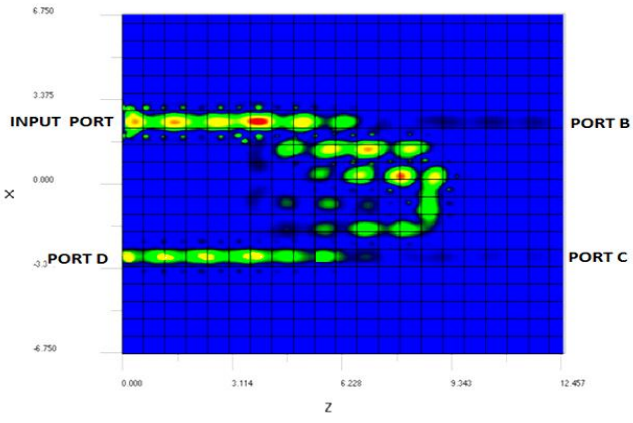

(b)

Fig. 3(a.) Electric field distribution Image Map for ADF (A). (b.) Electric field distribution Image Map for ADF (B)

Image maps show significant variation in the field distribution as backward dropping of the input light at the operating wavelength of 1.5 μm is shown. The difference

in behaviour of both the ADFs can be analyzed further with the help of transmittance curves as shown below in Fig. 4.

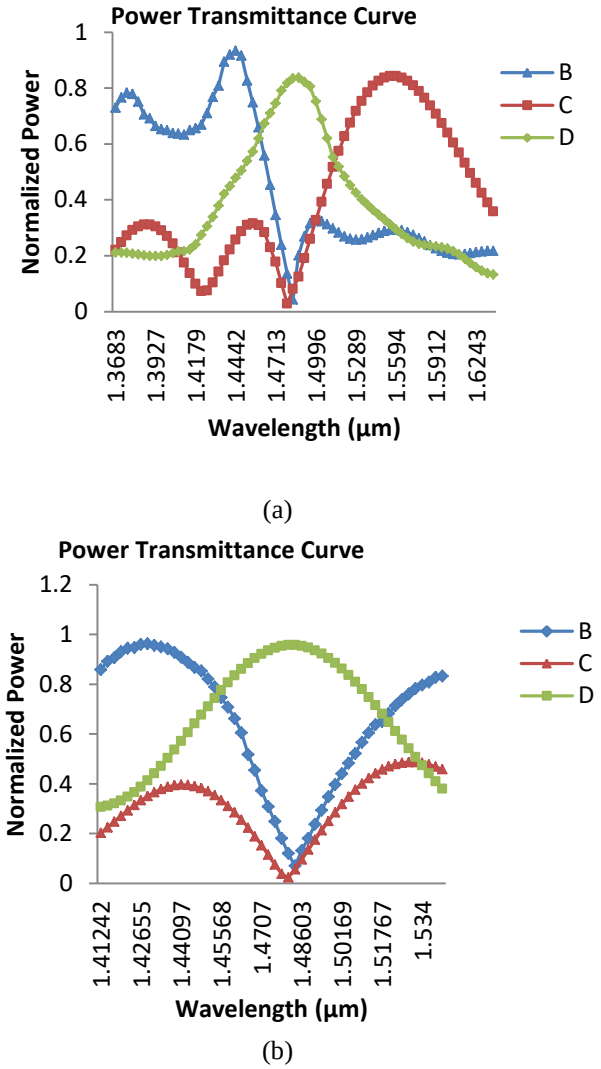

Fig. 4. (a) Power transmittance spectra for ADF (A). (b) Power transmittance spectra for ADF (B)

From the Fig. 4, it is observed that ADF (B) has better dropping efficiency than ADF (A). Maximum normalized power at the backward dropping wavelength for ADF configuration B is 95 %, whereas it is 83% for configuration A. However, the perfect power transfer takes place in both cases, i.e. at the wavelength (λ) equals to 1.483 µm, the output is obtained at port D with negligible transfer of light to the other ports. ADF (A) has spectral width of 68 nm for backward dropping whereas ADF (B) has 95 nm. Selectivity of ADF (A) is better than ADF (B) by 28%. ADF (A) has negligible transmission through port B after the wavelength is increased beyond 1.4478 µm. The light backward drops through the port D in the range 1.447 µm – 1.516 µm, and beyond it, light is completely transferred to the port C.

4. Conclusion

The two ADF configurations designed in this paper are analyzed using FDTD approach. The square cavity with multiple curved cavities inside is introduced in this design. The configuration ADF (A) has an output efficiency of 83% at the port D whereas spectral width of this configuration is 68 nm. And ADF (B) has an output efficiency of 95% at the port D but the spectral width of this configuration is 95 nm. Therefore, if coupling is improved to enhance the drop efficiency, the spectral width also increases. The perfect drop at resonant wavelength is observed in both add/drop filters. The size of the design is 12.4 µm × 12.4 µm which is suitable for integration in the miniature sized devices.

References

[1] E. Yablonovitch, Physical Review Letters **58**(20), 2059 (1987).
[2] J. D. Joannopoulos, R. D. Meade, J. N. Winn, Photonic Crystal: Modeling of Flow of Light, Princeton University Press, Princeton, 2005.
[3] B. Kumar, V. Suthar, K. S. Kumar, A. Singh, Progr. Electromag. Res. Lett. **33**, 27 (2012).
[4] Yu-Jun Quan, P. D. Han, Xiao-Dong Lu, Zhi-Cheng Ye, Li Wu, Optics Communications **27**, 203 (2007).
[5] C. J. Wu, M. H. Lee, W. H. Chen, T. J. Yang, J. Electromagnatic Waves Appl. **25**(10), 1360 (2011).
[6] S. Robinson, R. Nakkeeran, Optik **124**, 3430 (2013).
[7] Fu-Li Hsiao, Chengkuo Lee, SPIE J. Micro/Nanolith. MEMS MOEMS.**10**(1):013001, (2011).
[8] Ahmed Taalbi, Ghaouti Bassou, Mahmoud Youcef Mahmoud, Optik **124**, 824 (2013).
[9] P. Andalib, N. Granpayeh, IEEE **37**, 170 (2008).
[10] M. Djavid, M. S. Abrishamian, Optik **123**, 167 (2012).
[11] B. Painam, P. K. Teotia, R. S. Kaler, M. Kumar, in 12th International Conference on Fiber Optics and Photonics, OSA Technical Digest (online) (Optical Society of America, 2014), paper S5A.48.
[12] J. Jun-zhen, Q. Ze-Xuan, Z. Hao, Z. Yan-min, Q. Yi-Shen, Optoelectronics Letters **10**(1), 34 (2014).
[13] Y. Takahashi, T. Asano, D. Yamashita, S. Noda, Opt. Express **22**(4), 4692 (2014).
[14] J. J. V. Olmos, M. Tokushima, K. Kitayama, IEEE Journal of Selected Topics in Quantum Electronics **16**(1), 332 (2010).
[15] M. A. M. Birjandi, A. Tavousi, A. Ghadrdan, Elsevier, Photonics and Nanostructures-Fundamentals and Applications **21**, 44 (2016).
[16] J. B. Pendry, Journal of Physics: Condensed Matter **8**(9), 1085 (1996).
[17] A. Taflove, "Computational Electrodynamics: The Finite-Difference Time-Domain Method," Artech House, Boston, London, 2005.

*Corresponding author: harkiranjeet19@gmail.com